
In Vivo Detection of Stem Cells Grafted in Infarcted Rat Myocardium

Rong Zhou, PhD¹; Daniel H. Thomas, MD¹; Hui Qiao, PhD¹; Harshali S. Bal, BS¹; Seok-Rye Choi, PhD¹; Abass Alavi, MD¹; Victor A. Ferrari, MD^{1,2}; Hank F. Kung, PhD^{1,3}; and Paul D. Acton, PhD¹

¹Department of Radiology, University of Pennsylvania, Philadelphia, Pennsylvania; ²Cardiovascular Division, Department of Medicine, University of Pennsylvania, Philadelphia, Pennsylvania; and ³Department of Pharmacology, University of Pennsylvania, Philadelphia, Pennsylvania

The evaluation of stem cell-mediated cardiomyoplasty by non-invasive in vivo imaging is critical for its clinical application. We hypothesized that dual-tracer small-animal SPECT would allow simultaneous imaging of ^{99m}Tc-sestamibi to assess myocardial perfusion and of ¹¹¹In-labeled stem cells to delineate stem cell engraftment. **Methods:** Three to 4 million rat embryonic cardiomyoblasts (H9c2 cells) were labeled with 11.1–14.8 MBq (0.3–0.4 mCi) of ¹¹¹In-oxyquinoline and then injected into the border zones of infarcted myocardium of rats. ¹¹¹In images were acquired with a SPECT scanner 2, 24, 48, 72, and 96 h after the stem cells were injected into the infarcted myocardium. To visualize the perfusion deficit in the infarcted myocardium, we injected 74 MBq (2 mCi) of ^{99m}Tc-sestamibi (Cardiolite) intravenously 48 h after grafting. Dual-isotope pinhole SPECT was used to image ^{99m}Tc-sestamibi uptake simultaneously with ¹¹¹In to delineate retention of ¹¹¹In-labeled stem cells. The presence of labeled stem cells was confirmed by autoradiography and histology. **Results:** SPECT of ^{99m}Tc-sestamibi was used to delineate perfusion deficits and infarcted myocardium. Bull's-eye plots indicated that the ¹¹¹In signal from the labeled stem cells overlapped the perfusion deficits identified from the ^{99m}Tc-sestamibi images. The ¹¹¹In signal associated with the radiolabeled stem cells could be detected with SPECT of the heart for 96 h after engraftment. **Conclusion:** This study demonstrated the feasibility of using dual-isotope pinhole SPECT for high-resolution detection of perfusion deficits with ^{99m}Tc-sestamibi and with ¹¹¹In-labeled stem cells grafted into the region of the infarct.

Key Words: myocardium; ischemia; stem cells; indium; sestamibi; SPECT

J Nucl Med 2005; 46:816–822

Coronary heart disease is the leading cause of death in the United States. Postinfarction survival has improved in recent years because of the optimal therapies afforded by modern medicine. However, none of the therapies is able to

reverse the destructive cascade that occurs after acute myocardial infarction: loss of cardiomyocytes, development of myocardial fibrosis, subsequent left ventricular (LV) remodeling, progressive LV dilatation, and heart failure. In fact, according to studies by the American Heart Association, in up to 50% of patients who experience a moderate or larger infarction, progressive LV dysfunction may develop. A novel treatment strategy, often referred to as cellular cardiomyoplasty, includes local (intramyocardial or intracoronary) and systemic (intravenous) delivery of fetal or neonatal cardiomyocytes, skeletal myoblasts, or embryonic or bone marrow-derived stem cells. This strategy aims at enhancing cardiac function by repopulating the infarcted region with viable cardiomyocytes and, therefore, bears great promise for the cure of this disease (1).

Before stem cell-mediated cardiomyoplasty can be applied in the clinic, basic research must be performed using animal models to address critical issues: Do the grafted cells survive in sufficient numbers to be biologically meaningful? Can grafted cells differentiate into cardiomyocytes in response to local stimuli? Do the grafted cells contribute to the improvement of contractile function in addition to the improvement of global function? Survival of grafted cells has been evaluated by labeling cells with BrdU or fluorescent dye followed by detection of the labels in tissue samples, or by quantification of male DNA in the donor cells using real-time polymerase chain reaction technique (2–4). However, the invasive nature of the technique allows only a single time-point study for each animal; thus, information on the natural history of cell survival or proliferation in an individual animal is lost. The approach of using a reporter or marker gene holds promise for noninvasive quantification of cell survival. The survival fraction of grafted cells can be evaluated over time by stably transfecting cells with a reporter gene (e.g., HSV1-tk), and quantification of reporter gene expression by PET or SPECT would allow evaluation of survival fraction of grafted cells over time. The original work of developing HSV1-tk as a reporter gene was pioneered by Gambhir et al. (5,6) and Tjuvajev et al. (7). PET of rat cardiomyoblasts (H9c2 cells) that were grafted into rat

Received Jul. 22, 2004; revision accepted Jan. 16, 2005.

For correspondence or reprints contact: Paul D. Acton, PhD, 1 Silverstein, HUP, 3400 Spruce St., Department of Radiology, University of Pennsylvania, Philadelphia, PA 19104-4283.

E-mail: pacton@mail.med.upenn.edu

myocardium after being transfected by HSV1-tk has been reported recently (8). When the cells are transfected with another reporter gene, firefly luciferase (Fluc), bioluminescent imaging can be used for detection of these cells (9,10). Differentiation of stem cells can also be monitored noninvasively by imaging a tissue-specific reporter gene, such as Fluc, under the transcriptional control of the mouse ventricular myosin light chain 2 (MLC2v) gene, whose expression is primarily limited to cardiac ventricular myocardium in adult mice (11). Such a cardiac-specific reporter gene (MLC2v-Fluc) was used previously to study regulation of embryonic heart development in postmortem samples (12–14). In vivo detection of MLC2v-Fluc reporter gene expression by bioluminescent imaging has been achieved in mice recently (15).

Although optical (e.g., bioluminescence) and nuclear medicine (PET and SPECT) imaging modalities are sensitive for imaging gene expression, global cardiac function (e.g., ejection fraction and cardiac output) is routinely measured by MRI in the clinic because of the superior spatial resolution and tomographic acquisition method provided by MRI. Cardiac MRI of small animals (especially mice) at a high magnetic field strength (4–11 T) has greatly advanced in recent years (16–19), largely because of the wide application of transgenic models. MRI has yielded accurate and reliable quantification of murine global myocardium function (e.g., ejection fraction and cardiac output), LV mass, and right ventricular size (17,20,21). Cardiac wall motion and strain can be obtained by tagged MRI (18,22), a unique, noninvasive technique for evaluation of regional contractile function (23,24). In summary, noninvasive imaging techniques hold the key to addressing critical issues associated with stem cell therapy. Therefore, it is necessary to establish multimodality imaging as a means of investigating these complicated issues efficiently and accurately.

In this study, we attempted to use clinically applicable tracers for detection of stem cells in a rat model of myocardial ischemia (infarction) using ultra-high-resolution SPECT. We hypothesized that dual-tracer SPECT would allow simultaneous detection of perfusion deficits in the infarcted myocardium with ^{99m}Tc -sestamibi and of grafted stem cells labeled with ^{111}In .

MATERIALS AND METHODS

Rat Model of Myocardial Infarction

Male Sprague–Dawley rats (6–8 wk old, 220–250 g) were purchased from Charles River Laboratories. The animals were anesthetized by an intraperitoneal injection of ketamine and xylazine (50 and 2.5 mg/kg, respectively) and then were intubated and ventilated through a small-animal ventilator (model 680; Harvard Apparatus). The tidal volume (1.5–2.5 mL) was determined for each animal according to its respiratory rate and body weight. One percent isoflurane mixed with oxygen was used to maintain the anesthesia during surgery. The body temperature was maintained by a heating lamp. The electrocardiogram was monitored through-

out the surgery. After the thoracic cavity and pericardium had been opened, the left anterior descending coronary artery (LAD) was ligated by passing a piece of 6-0 silk suture underneath the vessel and the surrounding myocardium. A small piece of polyethylene tubing was used to ligate the artery without damaging it. Ligation was maintained for 45 min, and LAD perfusion was then restored. ^{111}In -labeled cells were injected in 4–5 locations surrounding the infarcted (pale) region, and the thoracotomy incision was closed. All animal procedures were approved by the Institutional Animal Care and Use Committee of the University of Pennsylvania.

^{111}In Labeling of Stem Cells

Rat embryonic cardiomyoblast H9c2 cells were obtained from American Type Culture Collection and were maintained in Dulbecco's modified Eagle medium (DMEM) supplied with 10% fetal bovine serum. Cells were labeled with ^{111}In -oxyquinoline (Amersham) following the procedures described by Cesano et al. (25). Briefly, 3–4 million cells were incubated with serum-free DMEM containing 11.1–14.8 MBq (0.3–0.4 mCi) of ^{111}In -oxyquinoline for 30 min. Cells were then washed 3 times with phosphate-buffered saline and resuspended in 200 μL of serum-free DMEM. Labeling efficiency was estimated by dividing the radioactivity of the cell suspension during incubation (total added activity) by the radioactivity of the cell suspension after washing (final activity) and multiplying by 100. These procedures resulted in labeling efficiency of around 85%.

SPECT Imaging

Cardiac SPECT was performed on a Prism 3000XP triple-head γ -camera (Philips Medical Systems) equipped with custom-made tungsten knife-edge pinhole collimators (Nuclear Fields) (26–28). The focal length of the collimators was 24 cm, with a radius of rotation of 5 cm and a pinhole diameter of 3 mm. The acquisition parameters included a continuous mode with 120 projection angles over a 360° arc to obtain data in a 128 \times 128 matrix with a pixel size and slice thickness of 3.56 mm. The images were then reconstructed using 10 iterations of a simultaneous algebraic reconstruction technique (29). Center of rotation error was corrected by scanning a thin line source and iteratively adjusting the center-of-rotation offsets until the reconstructed image was a point, rather than an annulus. The same source was used to measure the spatial resolution of the system for both ^{99m}Tc and ^{111}In . Images consisted of a matrix of 128 \times 128 \times 128 with an isotropic voxel size of 0.74 mm. Attenuation and scatter correction were not performed on the SPECT data.

Perfusion images were obtained 30 min after injection of 74 MBq (2 mCi) of ^{99m}Tc -sestamibi (Cardiolite; Bristol-Myers Squibb Medical Imaging, Inc.). The 140-keV photons from ^{99m}Tc were acquired simultaneously with the 247-keV photons from ^{111}In using 2 separate energy windows. This allowed the ^{99m}Tc -sestamibi perfusion images to be registered spatially with the ^{111}In images of the grafted stem cells.

Cross talk between the 2 isotopes into each energy window was measured by scanning the rats with each isotope separately. After injection of ^{111}In -labeled stem cells, the rats were scanned with both sets of energy windows, and downscatter from the ^{111}In into the ^{99m}Tc energy windows was counted. Similarly, the rats were injected with ^{99m}Tc -sestamibi and scanned with both energy windows, to measure any overlap from the low-energy ^{99m}Tc photons into the high-energy ^{111}In window.

^{111}In images were acquired 2, 24, 48, 72, and 96 h after grafting of labeled stem cells. Perfusion images were obtained 48 h (2 d) after stem cell grafting.

Image Analysis

Regions of interest were placed over the most intense area of ^{111}In uptake, and the counts were measured for each scan. After correction for radioactive decay of the isotope, the relative counts were plotted as a function of time to determine the washout rate.

The bull's-eye plots for each study were obtained by first reorienting the data into short-axis slices. Each short-axis slice was processed to obtain circumferential profiles of the maximum intensity along each ray—also known as maximum count circumferential profile. For each slice, 80 rays were generated and the maximum along each ray was computed. These profiles were arranged as concentric rings starting from the apical region at the center and basal region at the periphery to give the bull's-eye plot. In addition, both long- and short-axis slices were extracted to give representative images for each animal in the region of the infarct.

Autoradiography and Histology

H9c2 cells were prelabeled with superparamagnetic iron oxide (SPIO) particles. Briefly, SPIO containing ferumoxides injectable solution (Feridex; Berlex Laboratories) was mixed with culture medium (final iron concentration, 50 $\mu\text{g}/\text{mL}$), into which poly-L-lysine (molecular weight, 275 kDa; Sigma) was added (final concentration, 0.4 $\mu\text{g}/\text{mL}$). The cells were incubated with the labeling medium for about 20 h, followed by 3 washes and incubation overnight in fresh medium, before harvest for ^{111}In labeling. Three million cells were injected into a rat with chronic infarction (1 wk after myocardium infarction surgery) and a rat with fresh infarction (immediately after surgery). Both rats were sacrificed 2 h after injection of labeled cells. The heart was perfused retrograde through the aorta with 5 mL of saline and then frozen in a bath of dry ice and acetone. After equilibrium had been reached at -20°C , 10- μm sections were cut on a cryostat microtome (Hacker Instruments) and thaw-mounted on microscope slides (3 sections per slide). Tissue sections were air-dried at room temperature and exposed to Cronex MRF-34 film for 20 h. The exposed film was developed by a Kodak automatic film processor.

Sections adjacent to the autoradiographic sections were reserved for histologic analysis. For Prussian blue staining, slides were incubated with Perls' reagent, consisting of 2% potassium

ferrocyanide (Sigma-Aldrich Co.) in 23.4% HCl, for 30 min in a dark room, followed by counterstaining with nuclear fast red (Sigma-Aldrich Co.). In addition, morphologic analysis of the slides was used to identify stem cells, which tend to be rounder and to have larger nuclei.

RESULTS

The spatial resolution of the pinhole SPECT system in the configuration used for the rat studies was measured using a thin line source for both isotopes. At the center of the field of view, the resolution for $^{99\text{m}}\text{Tc}$ was 3.9 mm, whereas for the higher-energy photons from ^{111}In the resolution was degraded slightly to 4.6 mm, because of increased penetration at the pinhole edges. No energy window cross-talk was observed for either isotope—that is, no counts were recorded above background levels in the $^{99\text{m}}\text{Tc}$ energy window from pure ^{111}In , and vice versa.

Long- and short-axis views of the normal rat myocardium revealed uniform uptake of $^{99\text{m}}\text{Tc}$ -sestamibi (Figs. 1A and 1C). However, the myocardial infarct was delineated clearly by a perfusion deficit (Figs. 1E and 1G). Bull's-eye plots (Figs. 2) generated from the $^{99\text{m}}\text{Tc}$ -sestamibi images revealed uniform perfusion in normal myocardium (Fig. 2A, rat 3), whereas a region of perfusion deficit (dark blue) was detected in infarcted myocardium (Figs. 2C and 2E for rats 2 and 4, respectively). The perfusion deficit was localized primarily in the territory supplied by the LAD, that is, the anterior lateral wall (Fig. 2C), or in the apical region of the heart (Fig. 2E). This observation is consistent with the myocardial infarction model generated from LAD ligation and reperfusion. In addition, comparison of Figures 2C and 2E also reveals a smaller region of perfusion deficit in rat 2 than in rat 4. These 2 rats were reimaged with $^{99\text{m}}\text{Tc}$ -sestamibi SPECT 7 wk after infarction and then were euthanized. Triphenyl tetrazolium chloride (30) staining of the myocardium showed that the infarction volume was approximately 5% of the LV volume in rat 2 and 18% in rat 4. Although the infarction volume estimated at this late stage of infarction is likely to be smaller than the initial volume

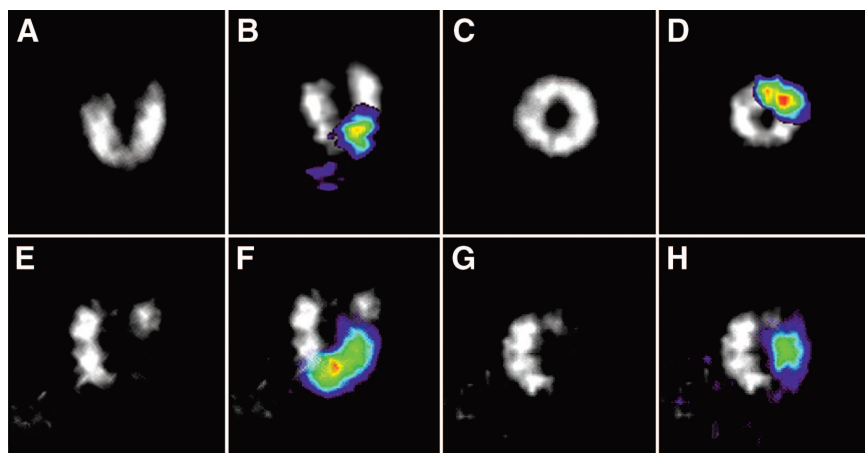


FIGURE 1. Cardiac long- and short-axis SPECT images of normal (A and C) and infarcted (E and G) heart using perfusion tracer $^{99\text{m}}\text{Tc}$ -sestamibi. ^{111}In signal (color) was overlaid on gray-scale $^{99\text{m}}\text{Tc}$ -sestamibi images for normal (B and D) and infarcted (F and H) heart.

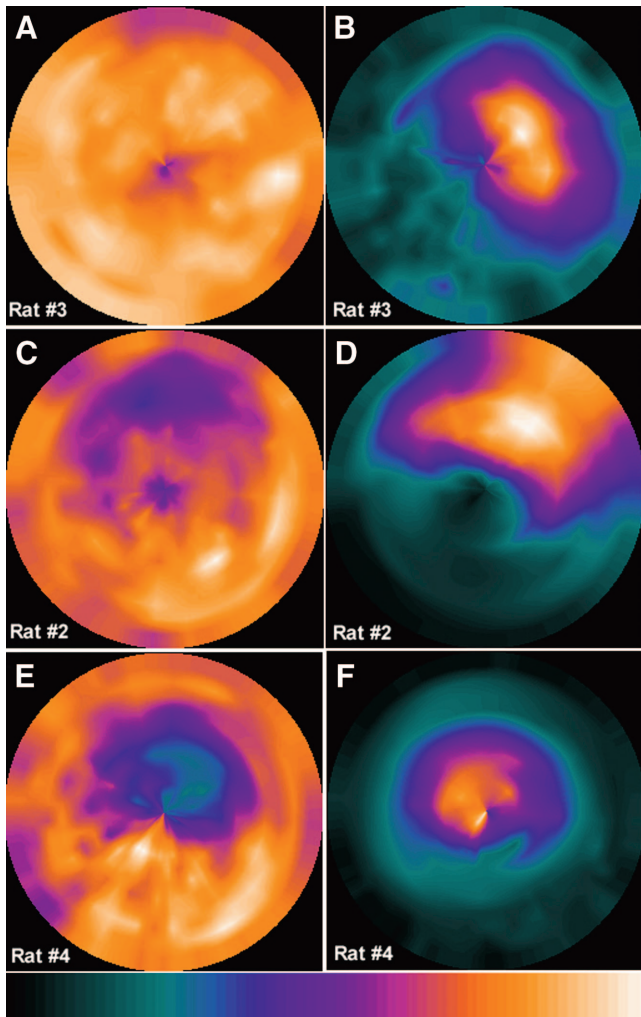


FIGURE 2. Bull's-eye plots of ^{99m}Tc -sestamibi signal (A, C, and E) and ^{111}In signal (B, D, and F) from normal rat (rat 3) and 2 rats with different infarction sizes (rats 2 and 4). Color bar represents transition from weak to strong signal intensity from left to right.

because of thinning of the infarcted myocardial wall, the difference in infarction size between the 2 animals was consistent with that observed from a qualitative visual inspection of the SPECT images.

Simultaneous detection of the 140-keV photons generated from decay of ^{99m}Tc and of the 247-keV photons from ^{111}In permits the perfect spatial coregistration of sestamibi and indium images. Because stem cells were injected both in normal rats and in rats with infarction, overlay of the ^{111}In signal (color) on the ^{99m}Tc -sestamibi image (gray scale) indicated that the ^{111}In signal coincided with the injection site in the normal rats (Figs. 1B and 1D) and also with the perfusion deficit region in the infarcted myocardium (Figs. 1F and 1H). Bull's-eye plots from the ^{111}In signal (Figs. 2B, 2D, and 2F) further confirmed this observation. The ^{111}In signal from rat 2 (Fig. 2D) was greater than that from rat 4 (Fig. 2F) because more ^{111}In activity (14.8 MBq [0.4 mCi]) was used to label the cells grafted in rat 2 than those grafted in rats 3 and 4 (11.1 MBq [0.3 mCi]).

The ^{111}In signal from the grafted stem cells was readily detected in the heart within 2 h after injection and remained detectable 96 h after injection. For visualization of washout of background ^{111}In signal from the lungs and thorax over time, a single transaxial slice at the level of the maximum ^{111}In uptake is shown in Figures 3A–3E for a normal rat (rat 3) and in Figures 3F–3J for a rat with infarction (rat 4). A threshold was applied to these images to give the same maximum pixel value in each. Uptake of ^{111}In in the thoracic region was observed in rat 3 within 2 h after grafting of stem cells but decreased to background levels 24 h after injection. Compared with rat 3, the background uptake of ^{111}In was minimal in rat 4, possibly because of a better injection with little or no leakage of radioactivity from the myocardium. Slight bleeding occurred in some animals during the injection (e.g., when the needle hit a capillary)

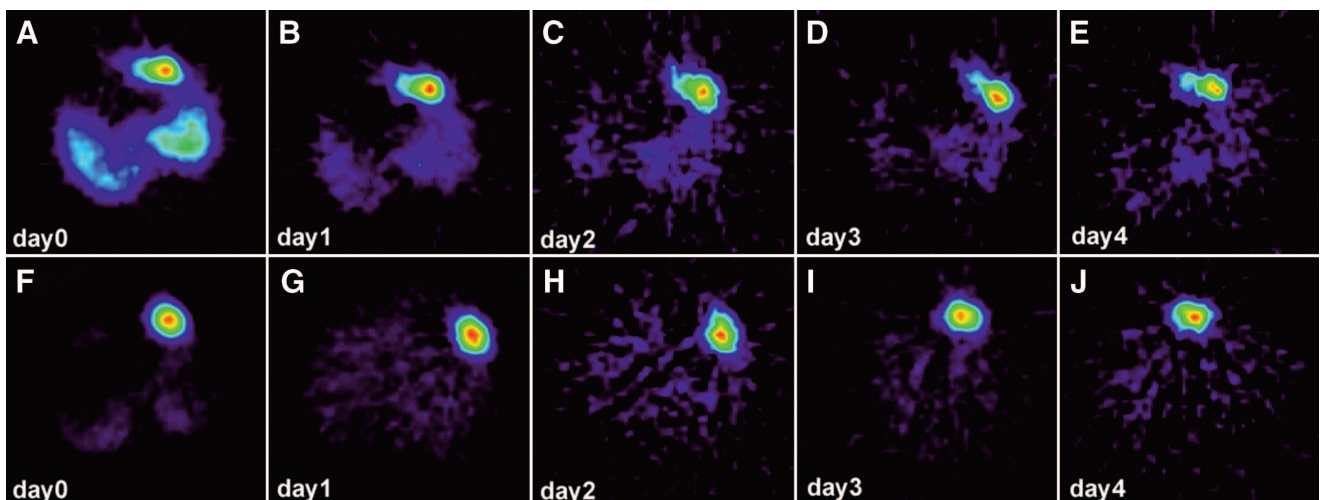


FIGURE 3. Time course of background ^{111}In signal intensity in region of lungs and thorax in rats 3 (top) and 4 (bottom). Each image was normalized to give same maximum count to show relative washout of tracer from thoracic cavity. Signal detected in thoracic region in rat 3 in first image (acquired within 2 h after injection) was likely due to some leakage during injection of cells.

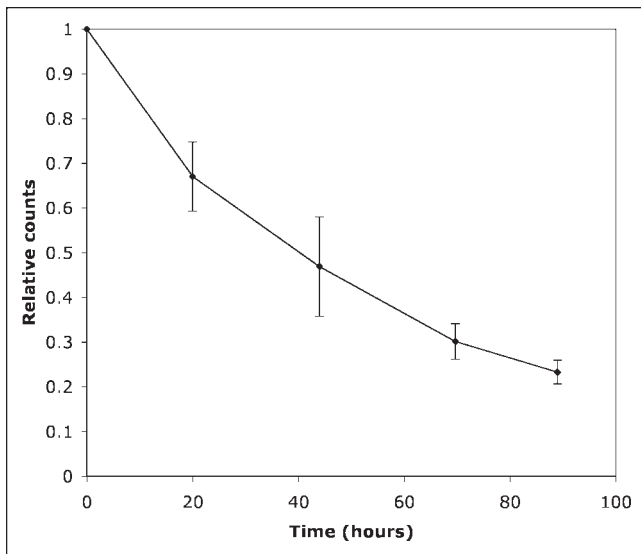


FIGURE 4. Time course of ¹¹¹In signal intensity in hearts from 6 animals. Curve was corrected for radioactive decay of ¹¹¹In. Error bars represent 1 SD.

and resulted in leakage of the injected cells from the injection site to the chest cavity.

Figure 4 shows the time course of the ¹¹¹In signal from the hearts of 6 animals ($n = 6$). The signal was normalized to the initial intensity of ¹¹¹In, acquired within 2 h after cell grafting. The mean washout half-life was 2.55 ± 0.09 d. This curve was corrected for the radioactive decay of ¹¹¹In (67.2-h half-life). Therefore, the curve reflects both clearance of the grafted stem cells from the myocardium and dissociation of the ¹¹¹In label from the grafted cells.

Autoradiographic images of ¹¹¹In uptake from 3 adjacent slices, with the corresponding photographs, are shown for rats 1 and 2 in Figures 5A and 5B. A region of intense ¹¹¹In uptake was identified on each slide. Histologic analysis (Fig. 5C) of adjacent slides confirmed SPIO-labeled cells in that region, where both intensely and lightly labeled cells were identified (Fig. 5D). The SPIO particles were stained

blue and localized in the cytoplasm. The injected cells had a unique morphology—round, with large nuclei stained red—which was different from the surrounding myocardium.

Some ¹¹¹In label in the autoradiographs, where no injected cells were found by histologic analysis, may represent free ¹¹¹In. This type of background was much lower in rat 1 than in rat 2, because the dose of ¹¹¹In used to label the cells was 50% less. Although a significant amount of blood was retained in the LV lumen (tissue photographs in Figs. 5A and 5B), the radioactivity was primarily mapped to the myocardial wall instead of to the blood. This was true for both rat 1 and rat 2 but was particularly clear in rat 2, which had a fresh infarction where the wall thickness remained unchanged. Rat 1 had a chronic infarction (1 wk old), and the LV wall in the infarcted region was much thinner.

DISCUSSION

¹¹¹In-Oxyquinoline and ^{99m}T-hexamethylpropylene amine oxime have been used routinely in the general nuclear medicine clinic for labeling autologous white blood cells, which are then infused back to the patients for localization of inflammatory sites and infectious foci (31,32). It is thought that the mechanism of labeling cells with ¹¹¹In-oxyquinoline involves an exchange between the oxyquinoline carrier and subcellular components that chelate indium more strongly than oxyquinoline. According to the manufacturer, approximately 24% of the radioactive label dissociates from the labeled leukocytes by 24 h. We are seeking possible chemical modifications of indium oxyquinoline so that the ¹¹¹In label of the cell is maintained longer than the physical decay (half-life, 67.2 h) of the radionuclide.

By incubation of 3–4 million cells with medium containing 11.1–14.8 MBq (0.3–0.4 mCi) of ¹¹¹In, labeled cells were detected up to 4 d after engraftment. By 96 h, about 20% of the injected dose (after correction for radioactive decay) remained around the infarction site. Because of the dissociation of ¹¹¹In from the labeled cells, the number of

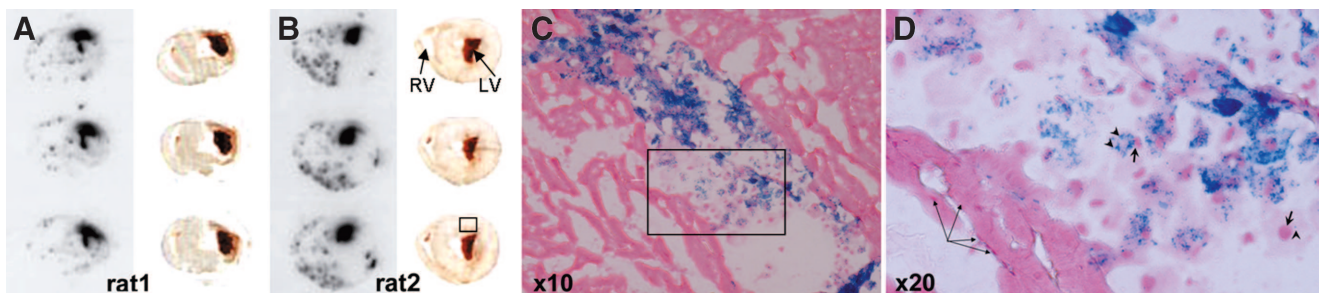


FIGURE 5. (A and B) Autoradiographs (left) of 3 adjacent slices and corresponding photographs (right). Region of intense ¹¹¹In uptake (boxed area) was identified on each slice. (C and D) Histologic analysis of adjacent tissue slices reveals injected cells localized in region outlined in box. SPIO particles (arrowheads) are stained blue, whereas nuclei (short arrows) are counterstained red. Magnified view (D) of boxed area in C shows intensely SPIO-labeled cells (e.g., 1 in center) and slightly labeled cells (e.g., 1 in right corner, which contained only 1 blue dot; the cell is round, as delineated by pink-stained cytoplasm, and has a large nucleus). Unique morphology distinguishes injected cells from surrounding myocardium. Bundle of muscle fibers (long arrows) is also seen. LV = left ventricle; RV = right ventricle.

cells that remained in the heart (where the radioactivity was counted) would have been greater than 20% of the initially grafted cells. The rest of the cells were removed from the heart through circulation or other mechanisms. Because the ^{111}In label may remain with the cell even after the cell has died, one cannot translate the observed radioactivity to the number of surviving cells. A marker gene approach (10,33) would be more suitable for estimating the survival fraction of injected stem cells, although the cells have to be transduced stably before they are grafted, a manipulation that may have a long-term effect on a cell. Therefore, ^{111}In is ideal for short-term tracking of cells and testing strategies that aim at enhancing the homing of stem cells. By being acquired simultaneously with ^{111}In , using different energy photons from the 2 tracers, the $^{99\text{m}}\text{Tc}$ -sestamibi images could localize the anatomic extent of normal perfused myocardium for registration with the ^{111}In images. The perfusion information provided by the $^{99\text{m}}\text{Tc}$ -sestamibi images potentially is useful for monitoring the functional recovery of infarcted myocardium in response to treatment.

The region where the injected cells (stained plus unstained) were found coincided with the hot region on the autoradiograph. Because the indium label could exit the cells, it is likely that free labels also contributed to some of the signal seen on both the in vivo SPECT images and the autoradiographs.

SPIO nanoparticles have been used to label stem cells (34,35), whose location was identified by MRI (36) after myocardial injection. The application of micrometer-sized SPIO particles (37) also has the potential to identify a few cells, or even a single cell, in situ. The magnetic field inhomogeneity generated by these particles induces a signal loss (void), not a signal enhancement as one would expect for a nuclear medicine tracer such as ^{111}In . Therefore, the specificity of this signal loss due to the presence of SPIO particles sometimes has to be verified. In addition, signals from surviving cells are not differentiated by this labeling technique from dead cells, or from macrophages that phagocytose the dead cells. A triple-labeling strategy might have the potential for monitoring short-term cell homing with ^{111}In , for monitoring long-term cell survival with reporter genes, and for defining anatomy and assessing migration of the cells with SPIO particles.

CONCLUSION

We demonstrated that ^{111}In -labeled cells were detected by ultra-high-resolution SPECT up to 96 h after they were grafted in the myocardium and that simultaneously acquired $^{99\text{m}}\text{Tc}$ -sestamibi images provided anatomic landmarks for localizing the ^{111}In distribution and for visualizing the perfusion deficit in the infarcted region.

ACKNOWLEDGMENTS

This research was supported by grants EB-002473, EB-000301, and EB-001809 from the National Institutes of

Health and by grant 0425558U from the American Heart Association. We thank Dr. Jeff W. Bulte for providing the method of stem cell labeling using Feridex.

REFERENCES

1. Reinlib L, Field L. Cell transplantation as future therapy for cardiovascular disease? A workshop of the National Heart, Lung, and Blood Institute. *Circulation*. 2000;101:E182-E187.
2. Reinecke H, Zhang M, Bartosek T, Murry CE. Survival, integration, and differentiation of cardiomyocyte grafts: a study in normal and injured rat hearts. *Circulation*. 1999;100:193-202.
3. Zhang M, Methot D, Poppa V, Fujio Y, Walsh K, Murry CE. Cardiomyocyte grafting for cardiac repair: graft cell death and anti-death strategies. *J Mol Cell Cardiol*. 2001;33:907-921.
4. Muller-Ehmsen J, Whittaker P, Kloner RA, et al. Survival and development of neonatal rat cardiomyocytes transplanted into adult myocardium. *J Mol Cell Cardiol*. 2002;34:107-116.
5. Gambhir SS, Bauer E, Black ME, et al. A mutant herpes simplex virus type 1 thymidine kinase reporter gene shows improved sensitivity for imaging reporter gene expression with positron emission tomography. *Proc Natl Acad Sci USA*. 2000;97:2785-2790.
6. Gambhir SS, Herschman HR, Cherry SR, et al. Imaging transgene expression with radionuclide imaging technologies. *Neoplasia*. 2000;2:118-138.
7. Tjuvajev JG, Chen SH, Joshi A, et al. Imaging adenoviral-mediated herpes virus thymidine kinase gene transfer and expression in vivo. *Cancer Res*. 1999;59:5186-5193.
8. Wu JC, Chen IY, Sundaresan G, et al. Molecular imaging of cardiac cell transplantation in living animals using optical bioluminescence and positron emission tomography. *Circulation*. 2003;108:1302-1305.
9. Contag PR, Olomu IN, Stevenson DK, Contag CH. Bioluminescent indicators in living mammals. *Nat Med*. 1998;4:245-247.
10. Wu JC, Inubushi M, Sundaresan G, Schelbert HR, Gambhir SS. Optical imaging of cardiac reporter gene expression in living rats. *Circulation*. 2002;105:1631-1634.
11. O'Brien TX, Lee KJ, Chien KR. Positional specification of ventricular myosin light chain 2 expression in the primitive murine heart tube. *Proc Natl Acad Sci USA*. 1993;90:5157-5161.
12. Lee KJ, Ross RS, Rockman HA, et al. Myosin light chain-2 luciferase transgenic mice reveal distinct regulatory programs for cardiac and skeletal muscle-specific expression of a single contractile protein gene. *J Biol Chem*. 1992;267:15875-15885.
13. Franz WM, Breves D, Klingel K, Brem G, Hofschneider PH, Kandolf R. Heart-specific targeting of firefly luciferase by the myosin light chain-2 promoter and developmental regulation in transgenic mice. *Circ Res*. 1993;73:629-638.
14. Meyer N, Jaconi M, Landopoulou A, Fort P, Puceat M. A fluorescent reporter gene as a marker for ventricular specification in ES-derived cardiac cells. *FEBS Lett*. 2000;478:151-158.
15. Gruber PJ, Li Z, Li H, et al. In vivo imaging of mlc2v-luciferase, a cardiac-specific reporter gene expression in mice. *Acad Radiol*. 2004;11:1022-1028.
16. Wiesmann F, Ruff J, Hiller K-H, Rommel E, Haase A, Neubauer S. Developmental changes of cardiac function and mass assessed with MRI in neonatal, juvenile, and adult mice. *Am J Physiol Heart Circ Physiol*. 2000;278:652-657.
17. Wiesmann F, Ruff J, Engelhardt S, et al. Dobutamine-stress magnetic resonance microimaging in mice: acute changes of cardiac geometry and function in normal and failing murine hearts. *Circ Res*. 2001;88:563-569.
18. Zhou R, Pickup S, Glickson JD, Scott C, Ferrari VA. Assessment of global and regional myocardial function in the mouse using cine- and tagged MRI. *Magn Reson Med*. 2003;49:760-764.
19. Thomas D, Ferrari V, Janik M, et al. Quantification of regional myocardial function after left ventricular infarction in rats. *Eur J Magn Reson*. In press.
20. Ruff J, Wiesmann F, Hiller KH, et al. Magnetic resonance microimaging for noninvasive quantification of myocardial function and mass in the mouse. *Magn Reson Med*. 1998;40:43-48.
21. Franco F, Dubois SK, Peshock RM, Shohet RV. Magnetic resonance imaging accurately estimates LV mass in a transgenic mouse model of cardiac hypertrophy. *Am J Physiol*. 1998;274:679-683.
22. Henson RE, Song SK, Pastorek JS, Ackerman JJ, Lorenz CH. Left ventricular torsion is equal in mice and humans. *Am J Physiol Heart Circ Physiol*. 2000;278:1117-1123.
23. Axel L, Dougherty L. Heart wall motion: improved method of spatial modulation of magnetization for MR imaging. *Radiology*. 1989;172:349-350.

24. Axel L, Dougherty L. MR imaging of motion with spatial modulation of magnetization. *Radiology*. 1989;171:841–845.
25. Cesano A, Visonneau S, Tran T, Santoli D. Biodistribution of human MHC non-restricted TALL-104 killer cells in healthy and tumor bearing mice. *Int J Oncol*. 1999;14:245–251.
26. Acton PD, Kung HF. Small animal imaging with high resolution single photon emission tomography. *Nucl Med Biol*. 2003;30:889–895.
27. Acton PD, Hou C, Kung MP, Plossl K, Keeney CL, Kung HF. Occupancy of dopamine D2 receptors in the mouse brain measured using ultra-high-resolution single-photon emission tomography and [123]IBF. *Eur J Nucl Med Mol Imaging*. 2002;29:1507–1515.
28. Acton PD, Choi SR, Plossl K, Kung HF. Quantification of dopamine transporters in the mouse brain using ultra-high resolution single-photon emission tomography. *Eur J Nucl Med Mol Imaging*. 2002;29:691–698.
29. Anderson AH, Kak AC. Simultaneous algebraic reconstruction technique (SART): a superior implementation of the ART algorithm. *Ultrason Imaging*. 1984;6:81–94.
30. Fishbein MC, Meerbaum S, Rit J, et al. Early phase acute myocardial infarct size quantification: validation of the triphenyl tetrazolium chloride tissue enzyme staining technique. *Am Heart J*. 1981;101:593–600.
31. Peters AM, Danpure HJ, Osman S, et al. Clinical experience with ^{99m}Tc-hexamethylpropylene-amineoxime for labelling leucocytes and imaging inflammation. *Lancet*. 1986;2:946–949.
32. Roddie ME, Peters AM, Danpure HJ, et al. Inflammation: imaging with Tc-99m HMPAO-labeled leukocytes: clinical experience with ^{99m}Tc-hexamethylpropylene-amineoxime for labelling leucocytes and imaging inflammation. *Radiology*. 1988;166:767–772.
33. Wu JC, Inubushi M, Sundaresan G, Schelbert HR, Gambhir SS. Positron emission tomography imaging of cardiac reporter gene expression in living rats. *Circulation*. 2002;106:180–183.
34. Bulte JW, Douglas T, Witwer B, et al. Magnetodendrimers allow endosomal magnetic labeling and in vivo tracking of stem cells. *Nat Biotechnol*. 2001;19:1141–1147.
35. Frank JA, Miller BR, Arbab AS, et al. Clinically applicable labeling of mammalian and stem cells by combining superparamagnetic iron oxides and transfection agents. *Radiology*. 2003;228:480–487.
36. Kraitchman DL, Heldman AW, Atalar E, et al. In vivo magnetic resonance imaging of mesenchymal stem cells in myocardial infarction. *Circulation*. 2003;107:2290–2293.
37. Hinds KA, Hill JM, Shapiro EM, et al. Highly efficient endosomal labeling of progenitor and stem cells with large magnetic particles allows magnetic resonance imaging of single cells. *Blood*. 2003;102:867–872.

Erratum

Table 3 in the article “Peptide Receptor Radionuclide Therapy for Non-Radioiodine-Avid Differentiated Thyroid Carcinoma,” by Teunissen et al. (*J Nucl Med*. 2005;46[suppl]:107S–114S), contained several errors. The corrected table appears below.

TABLE 3
Peptide Receptor Radionuclide Therapy in 58 Patients with Differentiated Thyroid Carcinoma

References	Tumor classification	Radiopharmaceutical			Cumulative dose	Response (TTP [mo])	Criteria*
		Radionuclide	Chelator	Peptide			
Gorges et al., 2001 (14)	3 × HCTC	⁹⁰ Y	DOTA	TOC	1.7–9.6 GBq	1 × SD (21), 2 × PD	NA
Waldherr et al., 2001 (15)	3 × FTC; 4 × PTC; 1 × ATC	⁹⁰ Y	DOTA	TOC	1.7–14.8 GBq	2 × SD (8,8); 6 × PD	WHO
Virgolini et al., 2002 (16)	25 × TC	⁹⁰ Y	DOTA	Lanreotide	0.9–7.0 GBq	3 × RD (NA), 11 × SD (NA), 11 × PD	WHO
Valkema et al., 2002 (17)	1 × FTC; 4 × PTC	¹¹¹ In	DTPA	Octreotide	29.5–83.2 GBq	4 × PD; 1 × SD (NA)	SWOG
Chinol et al., 2002 (21)	2 × PTC	⁹⁰ Y	DOTA	TOC	>7.4 GBq	NA	SWOG
Christian et al., 2003 (12)	1 × HCTC	⁹⁰ Y	DOTA	TOC	NA	NA	NA
Gabriel et al., 2004 (24)	4 × FTC; 1 × PTC	⁹⁰ Y	DOTA	TOC	5.6–7.4 GBq	5 × SD (5)	NA
Stokkel et al., 2004 (23)	4 × FTC; 5 × PTC	¹¹¹ In	DTPA	Octreotide	14.3–33.1 GBq	4 × SD; 5 × PD	NA

*WHO = World Health Organization criteria: regressive disease (RD) = >25% reduction in tumor size; SD = <25% reduction or increase in tumor size; PD = >25% increase in tumor size. SWOG = Southwest Oncology Group criteria of tumor response: PR = >50% reduction in tumor size; SD = ±25% reduction or increase in tumor size; PD = >25% increase in tumor size.

TC = undefined thyroid cancer; ATC = anaplastic thyroid carcinoma; NA = not available.